Supplementary figures

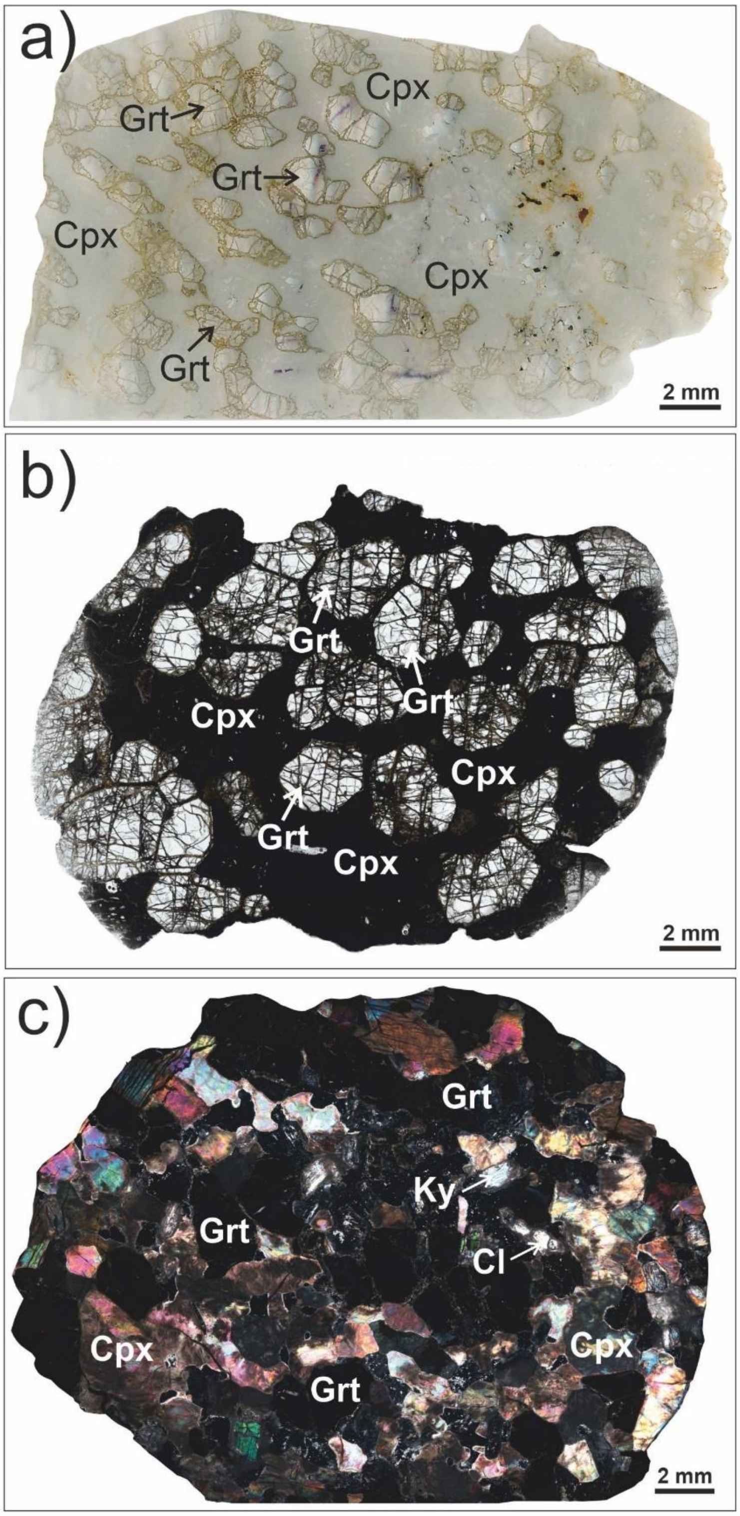

Fig. S1 Scanned thin section photomicrographs of eclogite xenoliths from the Wajrakarur Kimberlite Field (WKF), Eastern Dharwar craton. **(a)** Sample KL4-D2-6 (plane polarized light) shows the distribution of subhedral garnets (Grt) set in a matrix of mostly altered clinopyroxenes (clinopyroxene) with remnant clear cores. **(b)** Sample KL3-L (plane polarized light) shows coarse-grained granular texture, consisting of larger subhedral garnet grains distributed in a matrix of anhedral clinopyroxenes which appear dark due to extensive alteration. **(c)** Sample KL2-B1 (crossed polarized light) comprising garnet, partially altered clinopyroxene, and kyanite (Ky) along with secondary celsian (Cl)

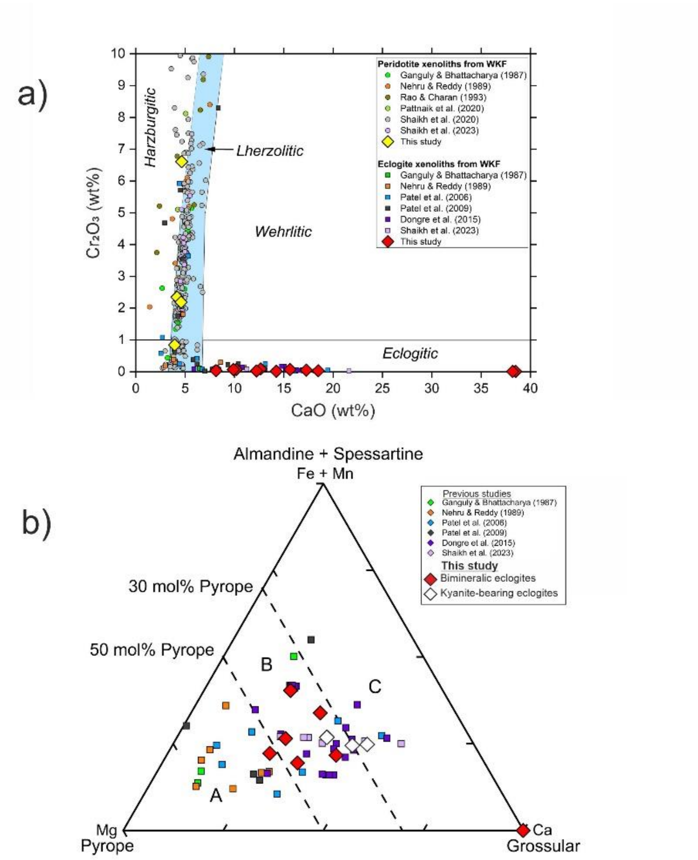

Fig. S2 (a) Cr_2O_3 (wt%) as a function of CaO (wt%) for garnet in eclogitic and peridotitic xenoliths in this study (yellow and red squares, respectively). The compositional fields of lherzolitic (light blue), harzburgitic, wehrlitic and eclogitic garnets are from Sobolev et al. (1973) **(b)** Ternary plot of molar (Fe+Mn)-Mg-Ca after Coleman et al. (1965) for garnet in eclogite xenoliths. Shown for comparison in both panels are samples from previous studies (Ganguly and Bhattacharya 1987; Nehru and Reddy 1989; Patel et al. 2006; Patel et al. 2009; Dongre et al. 2015; Shaikh et al. 2023) on the Eastern Dharwar craton as cited in the key

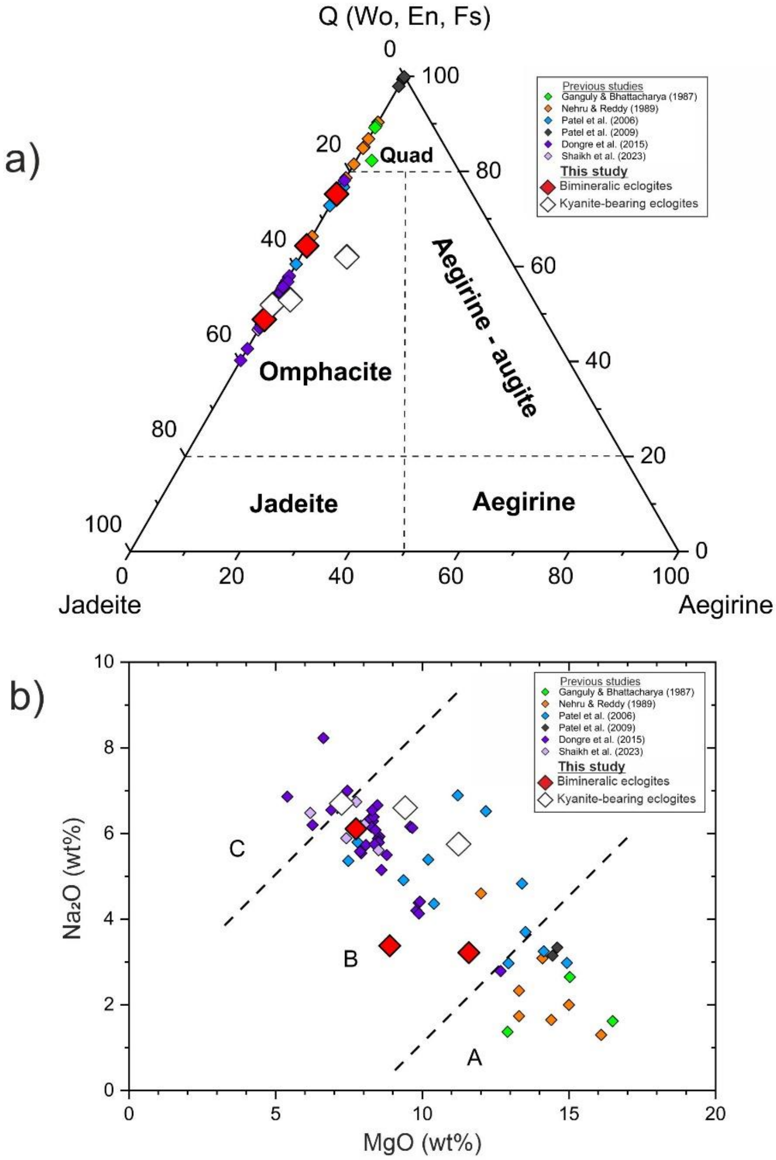

Fig. S3 (a) Compositions of clinopyroxene in eclogite xenoliths plotted on the end-member triangular diagram of Morimoto et al. (1989). Q = quadrilateral pyroxene; Wo = wollastonite; En = enstatite; Fs = ferrosilite **(b)** Na_2O content (wt%) as a function of MgO content (wt%) in clinopyroxenes. Subdivisions of Group A, B, and C eclogites are after Taylor and Neal (1989). Shown for comparison in both panels are samples from previous studies (Ganguly and Bhattacharya 1987; Nehru and Reddy 1989; Patel et al. 2006; Patel et al. 2009; Dongre et al. 2015; Shaikh et al. 2023) on the Eastern Dharwar craton as cited in the key

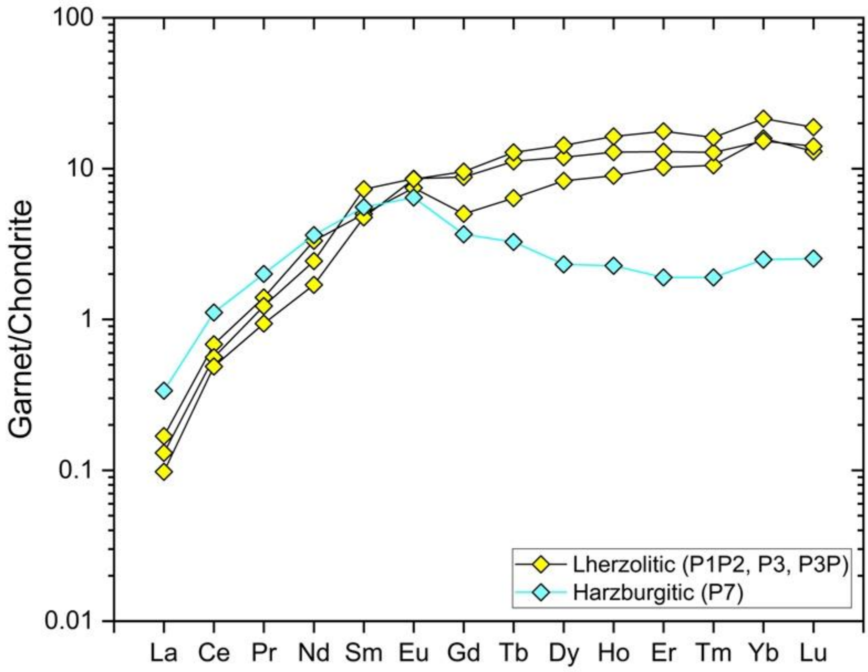

Fig. S4 Chondrite-normalized (McDonough and Sun 1995) REE pattern for peridotitic garnets analyzed in this study from the Eastern Dharwar Craton

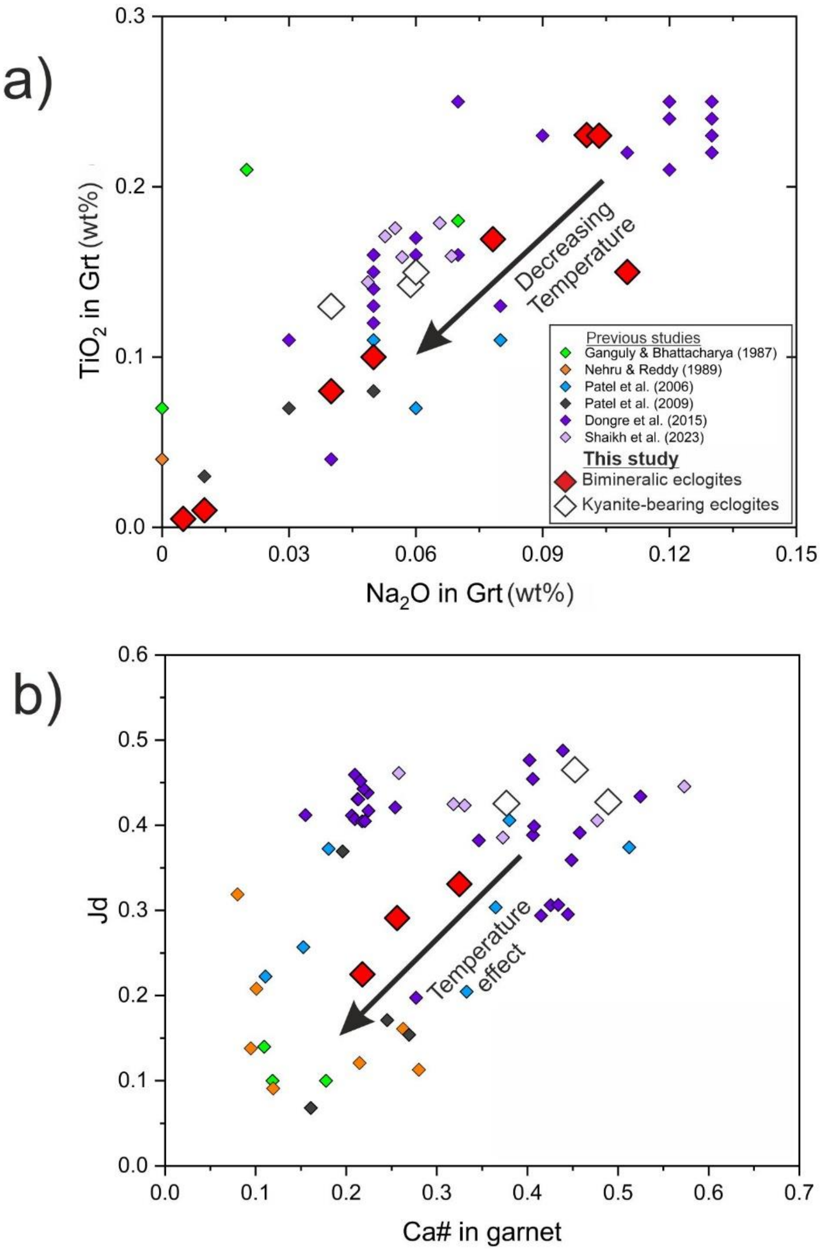

Fig. S5 (a) TiO_2 content (wt%) as a function of Na_2O content (wt%) in eclogitic garnet; the incorporation of both components is temperature-dependent, decreasing with decreasing temperature (Aulbach 2020), but would also be affected by metasomatism (bulk compositional effects). **(b)** Jadeite (Jd)-content in clinopyroxene as a function of grossular content [Ca# = Ca/(Ca + Fe + Mg + Mn)] in eclogitic garnet. With decreasing garnet Ca#, the jadeite component in the clinopyroxene also decreases in the Dharwar eclogites, which is a signature of metasomatism by kimberlite-like melt (Aulbach et al. 2020). Shown for comparison in both panels are samples from previous studies on the Eastern Dharwar craton as cited in the key

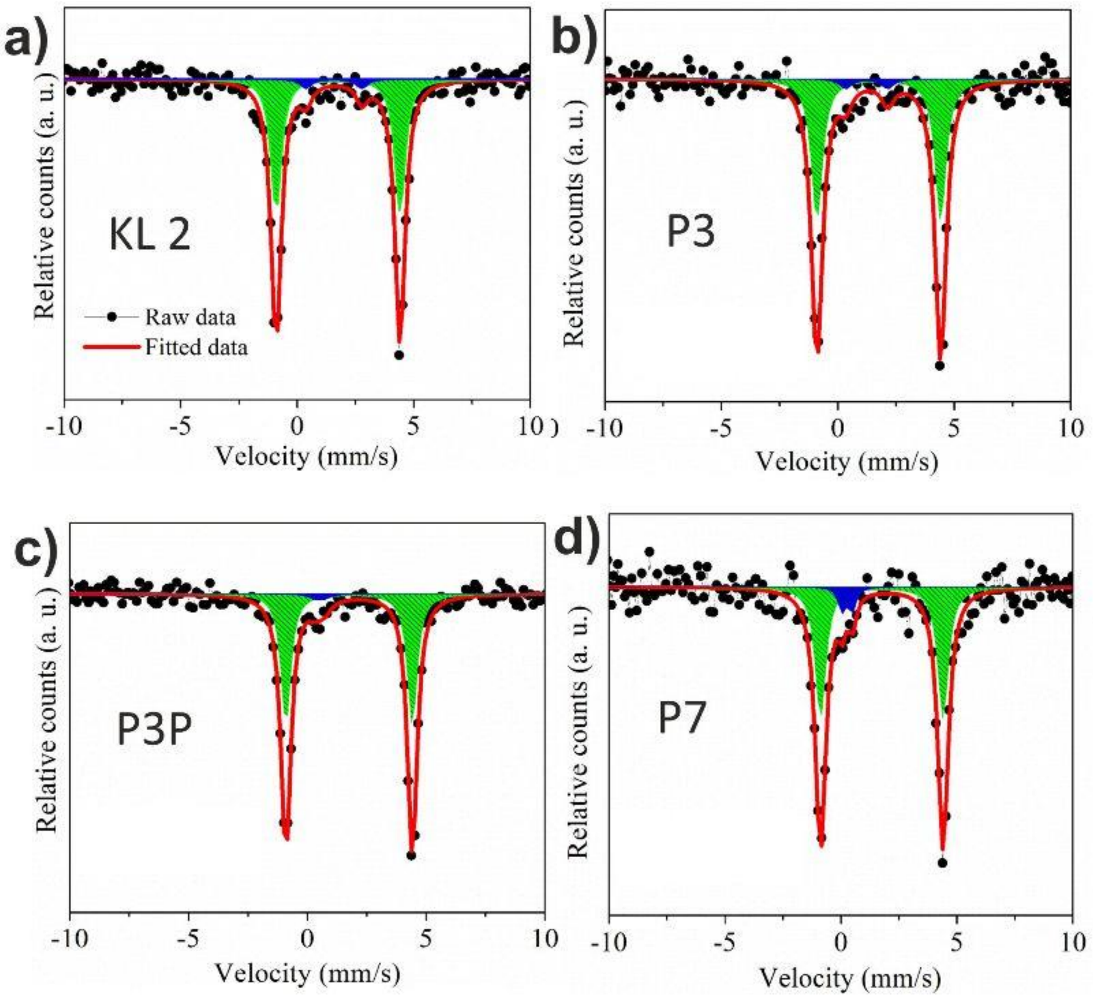

Fig. S6 Room-temperature ^{57}Fe Mössbauer spectra of eclogitic and peridotitic garnets from Wajrakarur kimberlites of the Eastern Dharwar craton. Panel **(a)** is an eclogitic garnet (sample KL-2) and panels **(b-d)** (samples P3, P3P and P7) are peridotitic garnets. $Fe^{3+}/\sum Fe$ is determined based on the relative areas of Fe^{3+} doublets (blue shaded areas)

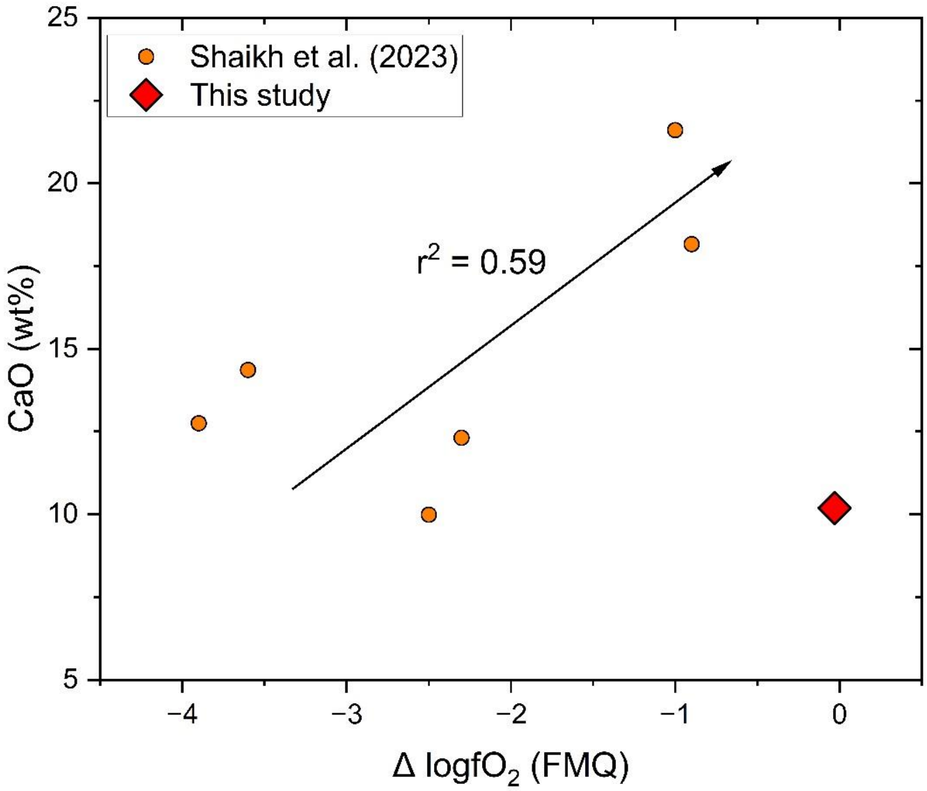

Fig. S7 CaO (wt%) plotted as a function of $\Delta\log fO_2$ [FMQ] for the eclogitic garnet from this study and compared with the data from previous study by Shaikh et al. 2023 from the Eastern Dharwar craton. The arrow (with regression through six samples from Shaikh et al. 2023) illustrates increasing silica-undersaturation in high-CaO eclogite xenoliths, resulting in fO_2 overestimation, rather than implying a true increase in oxygen fugacity with increasing CaO content (Aulbach et al. 2022)